Physics Letters B 711 (2012) 35–40

Contents lists available at SciVerse ScienceDirect

Physics Letters B

www.elsevier.com/locate/physletb

The astrophysical S factor of $^{12}C(\alpha,\gamma)^{16}O$ at stellar energy

D. Schürmann [a], L. Gialanella [a,b], R. Kunz [c], F. Strieder [d,*]

[a] Istituto Nazionale di Fisica Nucleare (INFN), Sezione di Napoli, I-80126 Napoli, Italy
[b] Dipartimento di Scienze Ambientali, Seconda Universitá di Napoli, I-81100 Caserta, Italy
[c] RUBION, Ruhr-Universität Bochum, D-44780 Bochum, Germany
[d] Institut für Experimentalphysik, Ruhr-Universität Bochum, D-44780 Bochum, Germany

ARTICLE INFO

Article history:
Received 10 October 2011
Received in revised form 22 March 2012
Accepted 25 March 2012
Available online 28 March 2012
Editor: V. Metag

Keywords:
Nuclear astrophysics
Helium burning
α-Capture reaction
Total S factor extrapolation

ABSTRACT

Stellar models show an exceptional sensitivity on the cross section of $^{12}C(\alpha,\gamma)^{16}O$ and a precision of about 10% is required to provide adequate constraints on stellar evolution. A measurement at the astrophysical energy, $E_0 \approx 300$ keV, is unfeasible due to the extremely low cross section. Furthermore, the extrapolation of existing high-energy data is complicated by a complex reaction scheme. Besides direct measurements of $^{12}C(\alpha,\gamma)^{16}O$, the β-delayed α-decay of ^{16}N and $^{12}C + {}^4He$ elastic scattering provide additional information for the relevant ^{16}O levels. In this Letter we present a new R-matrix analysis, where systematic uncertainties of the included data sets, in particular the absolute normalization, were treated in the fitting procedure. The data were selected according to rigorous criteria in order to reduce uncontrolled systematic effects and, finally, a Monte Carlo approach was used to evaluate the uncertainty at astrophysical energy. The resulting S factor, $S(300) = 161 \pm 19_{\text{stat}}{}^{+8}_{-2\,\text{sys}}$ keV b, is, for the first time, close to the required precision.

1. Introduction

In the first stage of stellar helium burning (stellar core temperature $T > 10^8$ K) the triple-α reaction is the dominating process, while later after build up of a significant carbon abundance the $^{12}C(\alpha,\gamma)^{16}O$ reaction is controlling this burning phase. Therefore, the helium burning time scale and the abundances of carbon and oxygen at the end of helium burning are determined by the $^{12}C(\alpha,\gamma)^{16}O$ cross section at the relevant Gamow energy of $E_0 \simeq 300$ keV [1,2]. The large uncertainties in the efficiency of convection induced mixing further complicate predictions of the central oxygen mass fraction [3,4]. Thus, an experimental determination of the $^{12}C(\alpha,\gamma)^{16}O$ cross section in the relevant energy region in the order of 10% or better will improve our understanding of the convection processes and remains one of the most important ingredients for the understanding of stellar evolution.

The cross section – usually expressed as the astrophysical S factor [5] – of the reaction $^{12}C(\alpha,\gamma)^{16}O$ ($Q = 7.162$ MeV) is dominated by E1 and E2 capture processes into the ^{16}O ground state. The two multipoles appear to be of similar importance and arise predominately from the high-energy tails of two subthreshold resonances at $E = -45$ ($J^\pi = 1^-$) and -245 keV (2^+),[1] and their interference with higher energy states of the same J^π (Fig. 1). The contribution of a direct capture process has to be considered for the E2 amplitude. Since the capture cross sections of the E1 and E2 multipoles have different energy dependencies, one must have an independent and precise information on each multipole cross section for an extrapolation to E_0. In addition to the ground state contributions cascade transitions have to be considered.

A detailed discussion of the various aspects of the determination of S(300) was presented in a review by Buchmann and Barnes [6]. Since then new information and data became available, in particular the total $^{12}C(\alpha,\gamma)^{16}O$ cross section data of Ref. [7]. Previous analyses were complicated by the considerable discrepancies in the absolute normalization of the direct $^{12}C(\alpha,\gamma)^{16}O$ experiments [8–22] carried out over the last almost 50 years. In the present new analysis these systematic effects were treated consistently by introducing a normalization factor as fit parameter. All individual contributions were fitted simultaneously with the constraint given by the total S factor considering the quoted systematic uncertainties of the various data sets. In addition, the information available from (α,α) elastic scattering and the β-delayed α-decay of ^{16}N were included. Subsequently, a Monte Carlo procedure was used to estimate the uncertainty on S(300). A data selection according to

* Corresponding author.
E-mail address: strieder@ep3.rub.de (F. Strieder).

[1] Energies are always in the center-of-mass system, except where quoted different.

0370-2693/$ – see front matter
http://dx.doi.org/10.1016/j.physletb.2012.03.064

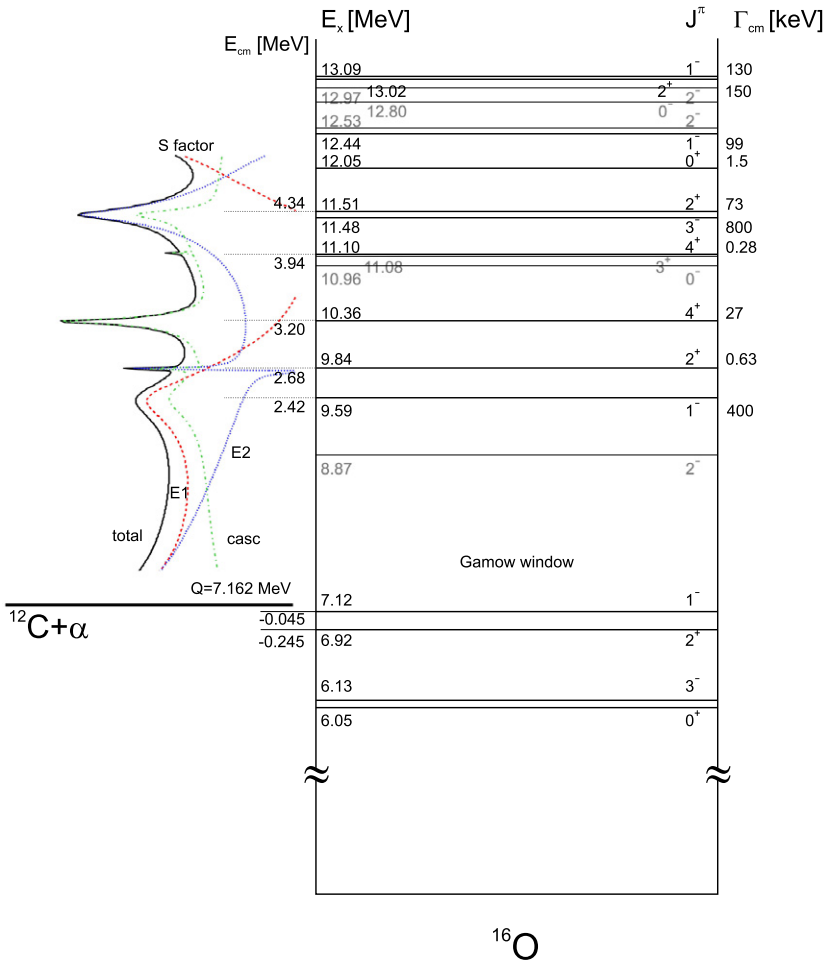

Fig. 1. Level scheme of the ^{16}O nucleus. All states relevant for the analysis are indicated. The energy dependence of the total S factor and its individual components are shown on the left.

the key requirements of the analysis was another important element and will be discussed below.

2. *R*-matrix analysis

The astrophysical S factor of $^{12}C(\alpha,\gamma)^{16}O$ at helium burning temperature has been derived in the R-matrix formalism. The corresponding R-matrix code was developed specifically for an analysis of this reaction and is based on an alternative parametrization [23] of the original R-matrix theory [24]. The code can use standard R-matrix parameters as well as physical resonance parameters [23] and is suited to fit simultaneously the direct γ-ray data, the ^{16}N β-delayed α-decay spectrum, and the (α,α) elastic scattering phase shifts, respectively. Radiative capture is included using internal and external contributions as in Barker and Kajino [25]. The details on the code will be published elsewhere [26].

The R-matrix calculations were performed for $J^\pi = 1^-$ and 2^+ (five levels each) and $J^\pi = 3^-$ and 4^+ (three levels each). A radius of $a = 5.5$ fm was used as suggested by [27]. The two 1^- states at $E_x = 12.44$ and 13.09 MeV are above the proton threshold and consequently the corresponding proton widths were included in the calculation. In a first step the resonance energies and α widths were fixed by a simultaneous fit to the phase shift and ^{16}N data. Subsequently, the γ-ray data were fitted together with the total capture cross section, and γ widths as well as the interference signs were obtained. Note, all possible interference sign combinations were tested and the combination resulting in the best overall fit of the capture data was selected for each transition.

2.1. Data selection

The γ-ray data sets included in the present R-matrix analysis were selected according to the following criteria: (a) an independent, well-documented absolute normalization with a corresponding uncertainty; (b) a sufficient angular resolution allowing for a reliable E1 and E2 separation, i.e. close geometry measurements have been excluded; (c) the data should span a broad energy range with a number of data points sufficient to constrain and test the S factor energy dependence; (d) a documentation on the target quality and an identification of background sources. As a general rule only published data sets were considered in this analysis, with the partial exception of the cascade data of the measurement of Kunz et al. [15]. These data are available from Ref. [28], but it is important to mention that the relevant experiment and data analysis have been peer reviewed in Ref. [15]. Moreover, these data were used for the extrapolation in Ref. [29].

The application of the selection criteria is straightforward in most cases like Refs. [9,10,12], where measurements were performed in close geometry, Refs. [11,13,14,18], where no independent normalization was determined, and Refs. [18,21], where only very few data in a narrow energy range were measured. Special attention deserves the widely used data of Redder et al. [11] and

Ouellet et al. [13], which have been excluded due to significant systematic ambiguities. The normalization of Ref. [13] was obtained at an energy where the corresponding experimental angular distribution is badly described by the expected theoretical distribution. This lack of internal consistency has already been noted previously [30]. In Ref. [11] the measurement of Dyer and Barnes [9] is used for normalization. However, from the documentation of the analysis [11] it is not clear if necessary corrections to the angular distribution, e.g. due to the finite size of the detectors, have been applied.

In general only few data sets exist on the cascade transitions. In addition to their overall normalization ambiguities, the cascade measurements of Refs. [10,11] are incompatible with each other, as noted in Ref. [6], and the presence of unresolved beam induced background is likely (e.g. see [28]). Thus, these two measurements were excluded from the analysis. The 6.05 MeV cascade data of Ref. [20] were discarded because of ambiguities in the identification of the individual cascade transitions in the experimental spectra (for details see Ref. [22]). Cascade transitions for energies $E > 3.3$ MeV have been reported recently in Ref. [22] and were used together with the low energy cascade data of Ref. [28]. A significant improvement compared to previous analysis was achieved including the total $^{12}C(\alpha,\gamma)^{16}O$ cross section data obtained with a recoil mass separator [7]. These data set a strong constraint on the sum of the different amplitudes.

The R-matrix analysis of $^{12}C(\alpha,\gamma)^{16}O$ is extremely sensitive to the ^{16}N β-delayed α-decay data and the phase shifts from (α,α) elastic scattering. The phase shifts for partial waves $l = 1$ to 4 were analyzed. The data of Tischhauser et al. [27,31] were used exclusively because in contrast to Refs. [32,33] the derived phase shifts do not show unphysical correlations. Finally, we considered the β-delayed α-decay spectrum of ^{16}N from Azuma et al. [34], where the data have adequate statistics and resolution, that is not the case in other experiments [35–38]. Note that there exists an ongoing discussion on the quality of the available ^{16}N data although Ref. [39] provided convincing arguments for the reliability of the data of Ref. [34].

In summary the data sets used simultaneously in the present R-matrix analysis were the phase shift data [31], the ^{16}N α spectrum [34], γ-ray data [15,16,19,22] and the total cross section data [7].

2.2. Treatment of systematic uncertainties

Systematic uncertainties in $^{12}C(\alpha,\gamma)^{16}O$ capture data have been considered previously only in the determination of the fit parameter uncertainties. The treatment of systematic uncertainties in the fitting procedure itself has been neglected. However, this may be extremely important in a simultaneous fit of a calculated R-matrix function to different data sets. These data are affected by different systematic errors, i.e. normalization uncertainties like detection efficiency, target thickness, ion beam current measurement, and charge state probability. Therefore, the normalization uncertainties influence the best fit and result in a biased estimate if neglected in the fitting procedure. In fact normalization errors determine a correlation between the uncertainties of the elements of each data set, and standard fitting procedures, e.g. χ^2 minimization for independent data, are inadequate. A proper treatment of normalization uncertainties is to fit uncorrelated data obtained by dividing each data set by an independent normalization factor [40]. These normalization factors should be fitted simultaneously and can be implemented defining a modified χ^2 for each component:

$$\chi^2 = \sum_i \left(\sum_j \frac{(c_i \cdot f(x_{i,j}) - y_{i,j})^2}{\sigma_{i,j}^2} + \frac{(c_i - 1)^2}{\sigma_{c_{\mathrm{exp},i}}^2} \right) \quad (1)$$

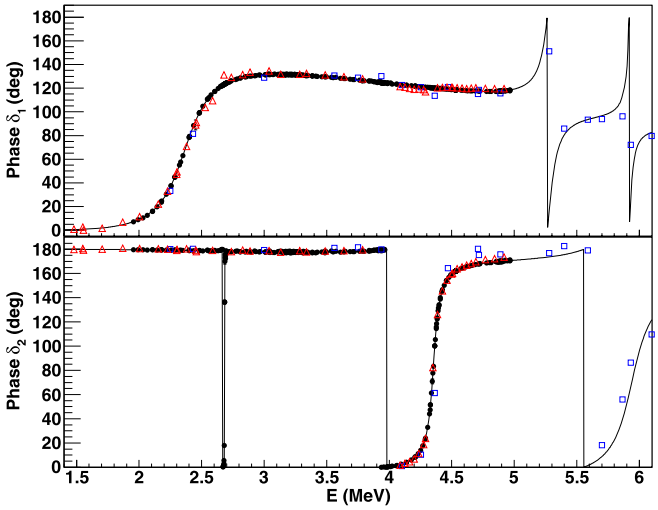

Fig. 2. Elastic scattering phase shifts from the present analysis (solid line) compared to experimental $l = 1$ (upper panel) and $l = 2$ (lower panel) data of Refs. [31] (full circles), [32] (open squares) and [33] (open triangles). The uncertainties are usually smaller than the symbols.

where $y_{i,j}$ represents the j-th data point of the i-th data set and $\sigma_{i,j}$ its uncertainty. The parameter c_i represents the inverse of a renormalization factor of the i-th data set, with an expectation value equal to 1 and uncertainty $\sigma_{c_{\mathrm{exp},i}}$ equal to the relative error on the normalization factor of the i-th data set. When a single experiment produced data for different components of $^{12}C(\alpha,\gamma)^{16}O$, the same normalization is used for all components as in the case of Refs. [15, 19]. Similarly, when different data sets are affected by the same uncertainty, the normalization is factorized into two contributions, i.e. an independent parameter and a second parameter common to both data sets.

3. Results

3.1. Elastic scattering and ^{16}N spectrum

In the analysis of elastic scattering phase shifts the Monte Carlo randomized phase shifts from Ref. [31] were used. The p-wave phase shift data and the β-delayed α spectrum of ^{16}N from Ref. [34] were fitted simultaneously. The energies of the subthreshold states were fixed to values from Ref. [41] while the reduced widths γ_α were fitted. The parameters of the 1^- levels at $E = 5.3$ and 5.9 MeV as well as the 2^+ level at 5.9 MeV were also kept to published values [41]. In the treatment of the ^{16}N α spectrum p- and f-wave contributions from the subthreshold 1^- and 3^- states, the 2.42 MeV 1^- level, and the 1^- background pole were included. For all other 1^- and 3^- levels the feeding amplitudes were set to zero. The α spectrum given by the R-matrix calculation was convoluted with a Gaussian function (FWHM = 30 keV) accounting for the detector resolution [34]. Like in [34] we excluded data in the energy range $E_\alpha = 1.98$ to 2.06 MeV from the analysis of the ^{16}N α spectrum due to a small contribution from the 2.68 MeV resonance in this energy window which represents a background for the analysis.

The best fits to the $l = 1$ and 2 phase shifts are shown in Fig. 2. The result is in good agreement with older phase shift data [32, 33] and the R-matrix parameters found in this work are in excellent agreement with the results given by [27]. Similarly to Ref. [31] a 5 keV energy shift for the 2.42 MeV 1^- resonance was observed with respect to the ^{16}N α spectrum. The fit to the ^{16}N α spectrum (Fig. 3) is of similar quality as in Ref. [34], with $\chi^2 = 101$ and

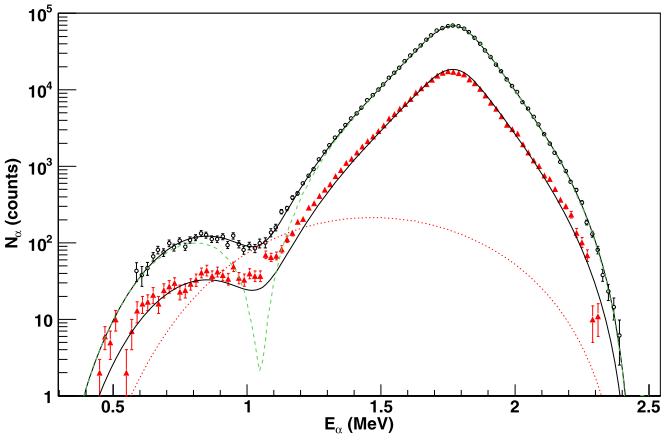

Fig. 3. Present best R-matrix fit (solid line) for the ^{16}N α spectrum from [34] (open circles) together with the decomposition into p- (dashed line) and f-wave (dotted line) contributions. For comparison, the data of [38] (full triangles) with the fit scaled by the corresponding number of observed α particles are shown.

100 for present and original analysis, respectively. In particular, independent fits to the individual data sets, i.e. the ^{16}N α spectrum and the p-wave phase shift data, showed that the α width of the 2.42 MeV 1^- resonance is in perfect agreement. A comparison of the best fit scaled to the α spectrum of Tang et al. [38] is also shown. Clearly a different shape with a larger width of the 2.42 MeV resonance is observed. In Ref. [39] it is speculated that this discrepancy originates from experimental difficulties. However, our result for the reduced α width of the 1^- subthreshold level, $\gamma_\alpha = 0.175$ MeV$^{1/2}$, is almost identical to the value from Ref. [38], $\gamma_{\alpha,\mathrm{Tang}} = 0.177$ MeV$^{1/2}$.

3.2. Gamma-ray data analysis

The results of the γ-ray data analysis and, thus, the extrapolation to S(300) have been obtained in a simultaneous fit of all capture data, including the total cross section data [7]. All narrow resonances in the total cross section data set were excluded and the R-matrix fit was performed with 32 fit parameters. Here we briefly report on the results for each transition. Full details will be given in a forthcoming extended publication [26].

The analysis of the E1 ground state transition includes 5 $J^\pi = 1^-$ levels: the $E_x = 7.12$ MeV subthreshold state, the first 3 states above the ^{12}C + α threshold, and a background pole. The fit parameters were the γ widths and the normalization coefficients. The γ width of the subthreshold state was fixed to the literature value [41], while Γ_γ of the 12.44 and 13.09 MeV states could vary within their literature uncertainties [41]. The selected E1 data sets [15,16,19] span essentially the range $1 < E < 3$ MeV, with increasing uncertainties on the low energy side. The present analysis including normalization uncertainties provided for the first time an excellent simultaneous fit to several E1 data sets (Fig. 4).

Similar to E1 the E2 ground state transition is dominated by a subthreshold state. This state as well as the first 3 states above threshold and a background pole formed the 5 level R-matrix employed in the analysis. In addition, a direct capture contribution is taken into account. The γ widths of the first two 2^+ states at $E_x = 6.92$ and 9.84 MeV were fixed to their literature values [41] while Γ_γ of the $E_x = 11.52$ and 13.02 MeV states were fit parameters. E2 ground state γ-ray data from Refs. [15,19,22] were used in the fit where data points in the energy range $2.62 < E < 2.72$ MeV were excluded in order to avoid influences from the narrow 2.68 MeV resonance. Note that the best fit resulted in an interference pattern of the 2.68 MeV resonance different from most previous analyses. This pattern is mainly determined by the high-energy data.

Transitions into the subthreshold states were previously assumed to make up a sizeable fraction of S(300) [20,42]. We analyzed transitions into all subthreshold states, i.e. $E_x = 6.05, 6.13, 6.92$ and 7.12 MeV. For all transitions we used the data of Ref. [22], while for the $E_x = 6.92$ and 7.12 MeV cascade transitions additional data from [28] were included. Since the cascade transitions are poorly understood, only few information are available on the cascade γ widths of the levels relevant to our analysis. Therefore, we treated the Γ_γ values as fit parameters, where the strategy was followed to keep the number of levels small.

For the transition into the $E_x = 6.05$ MeV excited state ($J^\pi = 0^+$) we followed the analysis of [22]. The E1 component is assumed to be negligible while for E2 the same level matrix as for the E2 ground state transition is employed. From the several

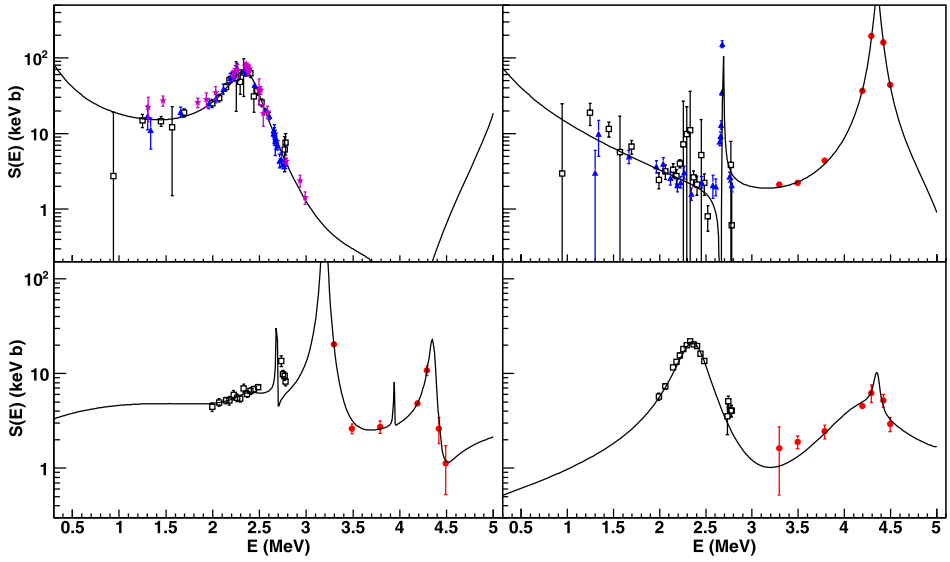

Fig. 4. Result of the E1 (upper left) and E2 (upper right) ground state components and the cascade transitions into the state at 6.92 MeV (lower left) and 7.12 MeV (lower right) of the R-matrix fit to all capture data. Data points shown are from Gialanella et al. [16] (stars), Kunz et al. [15,28] (open squares), Assunção et al. [19] (full triangles) and Schürmann et al. [22] (full circles).

similar interference combinations reported in [22] we selected a different one than in the previous work which is giving better results in the overall fits of all capture data. The S factor value $S_{6.05}(300) = 0.3$ keV b for this transition is negligible compared to $S_{\text{total}}(300)$.

Very little information exists about the transition into the $E_x = 6.13$ MeV state ($J^\pi = 3^-$). In particular no information on Γ_γ values are available. In the present analysis we have included E1 capture from the 4.34 MeV 2^+ resonance and E2 capture from the 4.32 MeV 3^- resonance. E2 direct capture may proceed through incoming p- and f-waves, respectively. These contributions were found to be sufficient to describe the experimental data of Ref. [22] and the fit resulted in $S_{6.13}(300) = 0.3$ keV b.

Capture into the $E_x = 6.92$ MeV state ($J^\pi = 2^+$) is dominated by E2 direct capture contributions from s-, d- and g-wave captures. The strength of the direct components is intimately related to the reduced α width of the final state which in our analysis is determined by the elastic scattering phase shifts. At higher energies this cascade transition is populated by the 3.20 MeV 4^+ and 4.34 MeV 2^+ resonances. We assumed capture through 1^- levels to be E1 and through 2^+ as well as 4^+ levels to be E2. Since no further information is present on the decay of 1^- levels to the $E_x = 6.92$ MeV state, only the γ widths of the 2.42 MeV resonance and the background pole were fit parameters, while the two higher lying 1^- levels were set to $\Gamma_\gamma = 0$. The two narrow resonances at 2.68 ($J^\pi = 2^+$) and 3.94 MeV ($J^\pi = 4^+$) were fixed to their literature values [41]. A good fit to the experimental data [22,28] was achieved with these parameters (Fig. 4) resulting in $S_{6.92}(300) = 3$ keV b. The data points around $E = 2.7$ MeV are clearly influenced by the narrow 2.68 MeV resonance and have been ignored. In an analysis by Buchmann [43] a value of $S_{6.92}(300) = 7$ keV b was reported. The main difference stems from the smaller 6.92 MeV 2^+ subthreshold width of $\gamma_{\alpha,\text{present}} = 0.47$ MeV$^{-1/2}$. Buchmann [43] found a value of $\gamma_\alpha = 0.75 \pm 0.15$ MeV$^{-1/2}$ based mainly on the cascade data of Redder et al. [11]. The present value, however, is in perfect agreement with the result of Ref. [27], $\gamma_\alpha = 0.47 \pm 0.06$ MeV$^{-1/2}$, which in turn is in excellent agreement with recent results from the analysis of transfer reaction measurements (see Table VI of Ref. [44] for details). Thus, this is the first time that the $^{12}C(\alpha,\gamma)^{16}O$ cascade transition, the phase shift and the transfer reaction analysis deliver consistent results.

The cascade transition through the 1^- level at $E_x = 7.12$ MeV is evident in the data around the broad 2.42 MeV 1^- resonance. We adopt E2 multipolarity for all transitions into this state from 1^- levels as reported in Ref. [11]. The γ widths of the 4.34 MeV 2^+ resonance (assuming E1 capture) as well as the 1^- background pole were fit parameters whereas for the 5.29 and 5.93 MeV levels the γ widths were fixed to literature values [41]. We further included the broad 4.32 MeV resonance ($J^\pi = 3^-$, assuming E2 capture) to explain the amplitudes seen around $E \simeq 4$ MeV. The γ width of the 3^- background pole was set to zero. In fact with these resonance parameters and the direct capture components (E2 from p- and f-wave capture) the observed energy dependence of the available data could be reproduced very well (Fig. 4). Possible transitions from the 4^+ levels would be of multipolarity E3 (or higher) and are therefore expected to be very weak. The extrapolated S factor for this transition is also small, $S_{7.12}(300) = 0.5$ keV b.

3.3. Total S factor and uncertainty determination

The final results are shown in Figs. 4 and 5. The total astrophysical S factor at helium burning temperature is $S(300) = 161.4$ keV b, and consists mostly of E1 ($S_{E1}(300) = 83.4$ keV b) and E2 ($S_{E2}(300) = 73.4$ keV b) ground state transitions with minor contributions from the cascade transitions, $S_{\text{casc}}(300) = 4.4$ keV b.

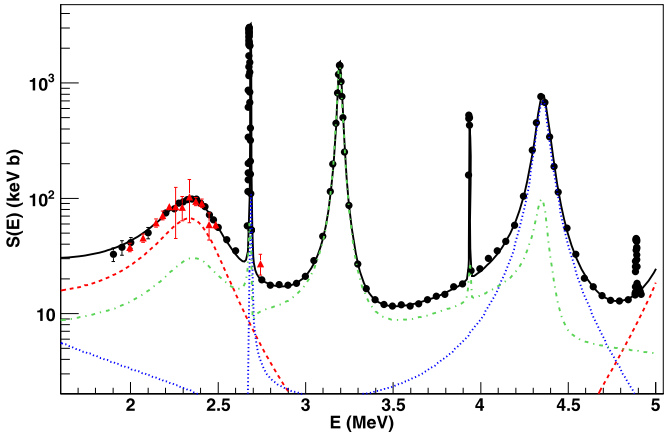

Fig. 5. Results of the R-matrix fit to all capture data. Shown are the sum of all components (solid line), and the decomposition into E1 (dashed line) and E2 ground state (dotted line) as well as the sum of all cascade transitions (dashed–dotted line). An excellent agreement with the total S factor data [7] (filled circles) and the sum of all transitions from Kunz et al. [15,28] (filled triangles) is achieved.

Table 1
Results of the simultaneous fit of all capture data. The resulting S(300) are given as a decomposition into the different transitions.

Transition	S(300) (keV b)	χ^2	Data sources	*ndp*[a]
tr → 0 (E1)	83.4	42.4	[15,16,19]	65
tr → 0 (E2)	73.4	71.3	[15,19,22]	42
tr → 6.05	0.3	3.3	[22]	7
tr → 6.13	0.3	1.4	[22]	7
tr → 6.92	3.3	17.9	[28,22]	19
tr → 7.13	0.5	18.7	[28,22]	19
Total[b]	161.4	69.4	[7]	77
Sum[c]	161.4	232.9[d]	[15,16,7,19,22,28]	243[d]

[a] Number of data points *ndp* in each χ^2 fit.
[b] Incoherent sum of all transitions compared to total cross section data [7].
[c] The 32-parameter fit of all transitions including χ^2 contributions from literature and normalization parameters.
[d] Contributions from normalization and literature comparison are included.

The best fits yield for the capture data $\chi^2_{\text{cap}} = 233$ (243 data points), the elastic scattering data, i.e. the sum for $l = 1$ to 4, $\chi^2_{\text{elast}} = 902$ (1416 data points), and the ^{16}N α spectrum $\chi^2_{^{16}N} = 100.7$ (87 data points). Table 1 summarizes the contribution of each capture transition to the total S factor and its χ^2 value, respectively. In a 1σ ($\Delta\chi^2_{1\sigma} \approx 21$) range of the corresponding χ^2_{cap} distribution we found several fits with other possible interference pattern leading to a S factor variation of $\Delta S(300) = {}^{+8}_{-2}$ keV b. This value was considered as a systematic uncertainty with respect to the choice of the interference signs.

In the past there have been several discussions on alternative interference combinations with substantial impact on S(300). The 1^- subthreshold state and the 2.42 MeV 1^- resonance may interfere destructively (see e.g. [13,16]) resulting in a significantly lower $S_{E1}(300)$. In the present work we would find $S_{E1(\text{destr})}(300) = 7.9$ keV b with $\chi^2_{\text{destr}} = 265$. Thus, the constructive solution is strongly favored and the destructive interference pattern has been rejected.

The main contributions to the total uncertainty arise from the α widths of the 1^- and 2^+ subthreshold states. The reduced α width of the 6.92 MeV 2^+ subthreshold state is strongly constrained by the elastic scattering phase shifts. The original analysis of Ref. [27] resulted in an uncertainty of about 13% on the α width. Such a large uncertainty, however, could not be reproduced in the current analysis, using the published phase shift data [31] only. These

phase shifts as well as the reduced α width of the subthreshold state were determined simultaneously in an R-matrix fit to experimental angular distributions. Thus, this method may introduce a correlation between the extracted values and subsequent R-matrix analyses. Since this cannot be clarified here and a fit of the original data is beyond the scope of the present work, we used the uncertainty quoted in Ref. [27] in our analysis.

Azuma et al. [34] reported that the ^{16}N α spectrum energy calibration is the largest contribution to the systematic uncertainty for the ^{16}N data, i.e. the 7.12 MeV 1^- subthreshold α width, leading to a 10% uncertainty in $S_{E1}(300)$. Such a variation in $S_{E1}(300)$ was found for a constant energy shift in the α spectrum of 2 keV. This value has been used as a 1σ standard deviation in the uncertainty estimation.

The uncertainty determination of the extrapolated S factor requires an error propagation of all relevant fit parameters through the fit function taking into account the covariances. That can be accomplished using a Monte Carlo approach as in Ref. [16], where the probability density distribution of S(300) is sampled by a repetitive fitting to pseudo data sets obtained distributing the original data according to the appropriate probability density distribution. Therefore, we generated pseudo data sets varying each data point according to a Gaussian distribution with standard deviation given by the experimental uncertainty. Similarly, the normalization constants of each data set were varied according to their experimental uncertainties. A Gaussian distributed set of values for S(300) was derived with this procedure resulting in $S(300) = 161 \pm 19$ keV b.

This is to our knowledge the first published analysis including total cross section data on $^{12}C(\alpha,\gamma)^{16}O$. In order to investigate the influence of the total cross section data on the results, we repeated the analysis neglecting these data. In this case the extrapolation of the E1 and E2 ground state transitions resulted in $S_{E1}(300) = 92$ keV b and $S_{E2}(300) = 76$ keV b, respectively, both larger than in the combined fit. Note that no effect on the selection of the interference pattern was observed. Finally, the uncertainty of S(300) is influenced by the total cross section data. Repeating the Monte Carlo uncertainty estimation without the total cross section data increased the 1σ uncertainty to $\Delta S(300)_{1\sigma} = 25$ keV b.

4. Summary and conclusion

The final result of $S(300) = 161 \pm 19_{\text{stat}}{}^{+8}_{-2\,\text{sys}}$ keV b represents the most precise analysis of the $^{12}C(\alpha,\gamma)^{16}O$ S factor at helium burning temperature presently available. This extrapolation is based on a set of complementary data including all available information which in addition have been reviewed according to clear and well-grounded criteria. For the first time normalization uncertainties have been explicitly included in the fit and the uncertainty on S(300) has been evaluated in a Monte Carlo procedure. The present S(300) matches the result of Kunz et al. [15], $S(300) = 165 \pm 50$ keV b, with a considerable smaller uncertainty and correct treatment of direct capture. In a recent review Buchmann and Barnes [6], a revision of Ref. [42], quote a value of $S(300) = 145$ keV b as the sum of all contributions, where significant discrepancies compared to the present evaluation are present for the E2 ground state ($S_{E2}(300) = 53^{+13}_{-18}$ keV b) and the cascade ($S_{6.05}(300) = 5^{+7}_{-4.5}$ keV b, $S_{6.92}(300) = 7^{+13}_{-4}$ keV b) contributions, respectively.

Note that some aspects still deserve further studies. The reduced α width of the 2^+ subthreshold state is presently constrained by the elastic scattering phase shifts. In view of the importance of this parameter for the E2 ground state contribution an independent estimate from capture γ-ray data would be highly desired. Unfortunately, the uncertainty and scattering on the E2 data are currently too large, which is a feature in all available analyses and expressed by the large χ^2. In the E1 ground state present data favor a constructive interference between 1^- subthreshold level and 2.42 MeV resonance. However, this is not yet fully conclusive, and only data with high precision and accuracy below $E = 1.3$ MeV would allow to exclude a destructive interference with high confidence.

Acknowledgements

The authors would like to thank F. Terrasi for many suggestions in statistics and data analysis, A. Di Leva, G. Imbriani, D. Rogalla, C. Rolfs, and O. Straniero for many inspiring discussions. This work was supported by DFG-Ro429/35 and INFN.

References

[1] G. Imbriani, M. Limongi, L. Gialanella, et al., Astrophys. J. 558 (2001) 903.
[2] M.F. El Eid, B.S. Meyer, L.-S. The, Astrophys. J. 611 (2004) 452.
[3] O. Straniero, I. Domínguez, et al., Astrophys. J. 583 (2003) 878.
[4] P.G. Prada Moroni, O. Straniero, Astron. Astrophys. 466 (2007) 1043.
[5] C. Rolfs, W. Rodney, Cauldrons in the Cosmos, University of Chicago Press, 1988.
[6] L.R. Buchmann, C.A. Barnes, Nucl. Phys. A 777 (2006) 254.
[7] D. Schürmann, A. Di Leva, et al., Eur. Phys. J. A 26 (2005) 301.
[8] J.D. Larson, R.H. Spears, Nucl. Phys. A 56 (1964) 497.
[9] P. Dyer, C.A. Barnes, Nucl. Phys. A 233 (1974) 495.
[10] K.U. Kettner, H.W. Becker, et al., Z. Phys. A 308 (1982) 73.
[11] A. Redder, H.W. Becker, C. Rolfs, et al., Nucl. Phys. A 462 (1987) 385.
[12] R.M. Kremer, C.A. Barnes, et al., Phys. Rev. Lett. 60 (1988) 1475.
[13] J.M.L. Ouellet, M.N. Butler, et al., Phys. Rev. C 54 (1996) 1982.
[14] G. Roters, C. Rolfs, et al., Eur. Phys. J. A 6 (1999) 451.
[15] R. Kunz, M. Jaeger, A. Mayer, et al., Phys. Rev. Lett. 86 (2001) 3244.
[16] L. Gialanella, D. Rogalla, F. Strieder, et al., Eur. Phys. J. A 11 (2001) 357.
[17] M. Fey, PhD thesis, Universität Stuttgart, Germany, 2004.
[18] R. Plag, M. Heil, et al., Nucl. Phys. A 758 (2005) 415.
[19] M. Assunção, M. Fey, et al., Phys. Rev. C 73 (2006) 055801.
[20] C. Matei, L. Buchmann, et al., Phys. Rev. Lett. 97 (2006) 242503.
[21] H. Makii, Y. Nagai, T. Shima, et al., Phys. Rev. C 80 (2009) 065802.
[22] D. Schürmann, A. Di Leva, et al., Phys. Lett. B 703 (2011) 557.
[23] C.R. Brune, Phys. Rev. C 66 (2002) 044611.
[24] A.M. Lane, R.G. Thomas, Rev. Mod. Phys. 30 (1958) 257.
[25] F.C. Barker, T. Kajino, Aust. J. Phys. 44 (1991) 369.
[26] R. Kunz, D. Schürmann, et al., 2012, in preparation.
[27] P. Tischhauser, R.E. Azuma, et al., Phys. Rev. Lett. 88 (2002) 072501.
[28] R. Kunz, PhD thesis, Universität Stuttgart, 2002.
[29] R. Kunz, M. Fey, et al., Astrophys. J. 567 (2002) 643.
[30] C.R. Brune, Phys. Rev. C 64 (2001) 055803.
[31] P. Tischhauser, A. Couture, et al., Phys. Rev. C 79 (2009) 055803.
[32] M. D'Agostino Bruno, et al., Nuovo Cimento Ser. A 27 (1975) 1.
[33] R. Plaga, H.W. Becker, et al., Nucl. Phys. A 465 (1987) 291.
[34] R.E. Azuma, L. Buchmann, et al., Phys. Rev. C 50 (1994) 1194.
[35] Z. Zhao, R.H. France III, et al., Phys. Rev. Lett. 70 (1993) 2066.
[36] R.H. France III, E.L. Wilds, et al., Phys. Rev. C 75 (2007) 065802.
[37] X.D. Tang, K.E. Rehm, et al., Phys. Rev. Lett. 99 (2007) 052502.
[38] X.D. Tang, K.E. Rehm, et al., Phys. Rev. C 81 (2010) 045809.
[39] L. Buchmann, G. Ruprecht, C. Ruiz, Phys. Rev. C 80 (2009) 045803.
[40] G. D'Agostini, Nucl. Instrum. Methods A 346 (1994) 306.
[41] D.R. Tilley, H.R. Weller, C.M. Cheves, Nucl. Phys. A 564 (1993) 1.
[42] L. Buchmann, R.E. Azuma, et al., Phys. Rev. C 54 (1996) 393.
[43] L. Buchmann, Phys. Rev. C 64 (2001) 022801.
[44] M. Dufour, P. Descouvemont, Phys. Rev. C 78 (2008) 015808.